Stem Cell Research & Therapy

RESEARCH

Open Access

Knockout of B2M in combination with PD-L1 overexpression protects MSC-derived new islet β cells from graft rejection in the treatment of canine diabetes mellitus

Pengxiu Dai[1], Yi Wu[1], Qingjie Du[1], Juanjuan Du[1], Keyi Wang[1], Ruiqi Chen[1], Xiancheng Feng[1], Chen Chen[2,3] and Xinke Zhang[1*]

Abstract

Background The immunogenicity of allogeneic mesenchymal stem cells (MSCs) is significantly enhanced after transplantation or differentiation, and these cells can be recognized and cleared by recipient immune cells. Graft rejection has become a major obstacle to improving the therapeutic effect of allogeneic MSCs or, after their differentiation, transplantation in the treatment of diabetes and other diseases. Solving this problem is helpful for prolonging the time that cells play a role in the recipient body and for significantly improving the clinical therapeutic effect.

Methods In this study, canine adipose-derived mesenchymal stem cells (ADSCs) were used as seed cells, and gene editing technology was used to knock out the B2M gene in these cells and cooperate with the overexpression of the PD-L1 gene. Gene-edited ADSCs (GeADSCs), whose biological characteristics and safety are not different from those of normal canine ADSCs, have been obtained.

Results The immunogenicity of GeADSCs is reduced, the immune escape ability of GeADSCs is enhanced, and GeADSCs can remain in the body for a longer time. Using the optimized induction program, the efficiency of the differentiation of GeADSCs into new islet β-cells was increased, and the maturity of the new islet β-cells was increased. The immunogenicity of new islet β-cells decreased, and their immune escape ability was enhanced after the cells were transplanted into diabetic dogs (the graft site was prevascularized by the implantation of a scaffold to form a vascularized pouch). The number of infiltrating immune cells and the content of immune factors were decreased at the graft site.

Conclusions New islet β-cell transplantation, which has low immunogenicity, can reverse diabetes in dogs, and the therapeutic effect of cell transplantation is significantly enhanced. This study provides a new method for prolonging the survival and functional time of cells in transplant recipients and significantly improving the clinical therapeutic effect.

Keywords Gene-edited ADSCs, Immunogenicity, New islet β cells, Antigraft rejection, Therapeutic effect

*Correspondence:
Xinke Zhang
zxk19830521@163.com
Full list of author information is available at the end of the article

Graphical abstract

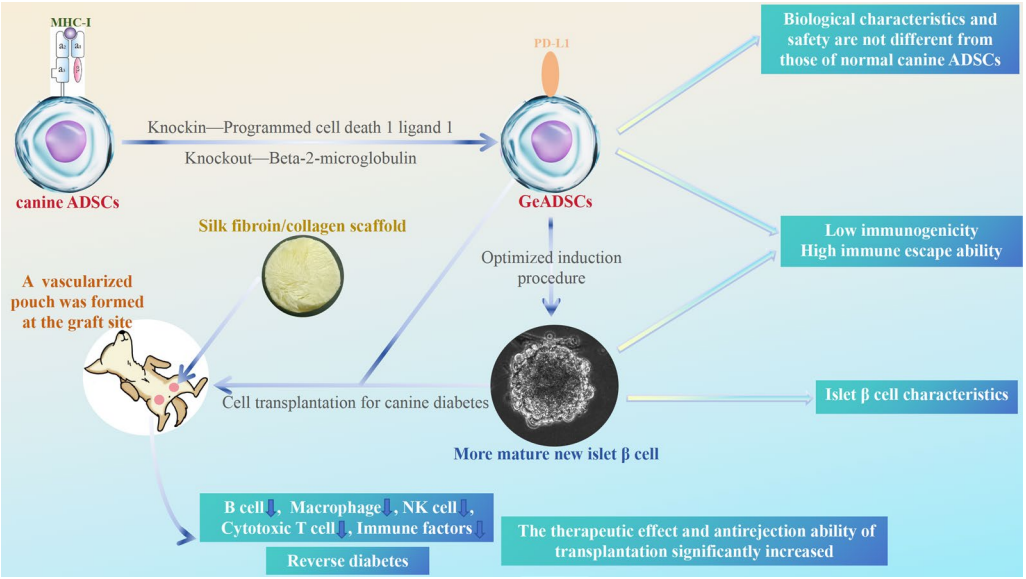

Introduction

Islet transplantation is an ideal way to treat insulin-dependent diabetes mellitus. However, the limited source of islet donors, complicated separation and purification procedures and immune rejection after transplantation greatly limit its clinical application ([8, 27]. Therefore, the search for islet replacement cell transplantation for the treatment of insulin-dependent diabetes has become the focus of current research. Allogeneic MSCs are derived from a wide range of sources, have multiple differentiation potentials, immunomodulatory functions and the ability to promote the repair of damaged tissues; and are ideal seed cells for cell transplantation therapy and tissue engineering [18, 26]. Allogeneic MSCs can be induced into insulin-producing cells (IPCs) in vitro by simulating the development environment of islet β-cells and changing the composition of the medium. In previous studies, highly effective regulatory gene combinations of 6 genes obtained by screening were used to differentiate canine allogeneic MSCs into new islet β-cells, which can be used for the treatment of canine diabetes mellitus. However, in the treatment of canine diabetes mellitus by cell transplantation, the therapeutic effect is not ideal because of graft rejection [6]. Graft rejection has become a major obstacle to improving the therapeutic effect of allogeneic MSCs or, after their differentiation, transplantation in the treatment of diabetes and other diseases. The improvement of the graft rejection problem can help prolong the survival and functional time of allogeneic MSCs or after their differentiation in transplant recipients and significantly improve the clinical effect of cell transplantation in the treatment of diabetes and other diseases.

Allogeneic MSCs have low immunogenicity in vitro, but their immunogenicity is significantly enhanced after transplantation in vivo. While the cells continue to play therapeutic and immunomodulatory roles, they can be recognized and cleared by the immune cells of the transplanted recipients. In particular, after the differentiation of allogeneic MSCs, their immunogenicity is significantly enhanced, and the transplanted cells are also cleared more quickly [38, 21, 30]. After allogeneic MSCs or after their differentiation are transplanted, graft rejection may be caused by a change in the phenotype of the transplanted cells. Although it has been reported that allogeneic MSCs exhibit immunomodulatory properties both in vitro and after transplantation, an increasing number of researchers believe that allogeneic MSCs do not have immune privilege characteristics, their immunogenicity cannot be ignored, and allogeneic immune rejection is inevitable [33, 35]. Cells transplanted in vivo can be recognized and cleared by the recipient's immune system while promoting the repair of damaged tissues [2]. When allogeneic MSCs are exposed to an inflammatory environment in vivo, MHC-I and MHC-II molecules are highly expressed, and their immunogenicity is significantly increased, which leads to immune rejection in transplant recipients. Repeated injections of allogeneic MSCs can lead to both primary and secondary humoral

reactions [1]. The immunogenicity of allogeneic MSCs can be decreased by knocking out MHC-I molecules on the cell surface [4]. The *B2M* (beta-2-microglobulin) gene encodes β2 microglobulin, which is an important subunit of MHC-I and is crucial for the structural stability and function of MHC-I. Its absence affects normal folding and transport to the cell surface of MHC-I [34]. In previous studies, we generated allogeneic MSC-B2M gene knockout strains, which showed decreased immunogenicity and improved antigraft rejection ability. However, since MHC-I is a ligand of the NK cell-killing inhibitory receptor, the deletion of MHC-I can activate NK cells and kill the allogeneic MSC-B2M knockout strain by NK cells after transplantation in vivo [10]. Therefore, it is necessary to further solve the problem of graft rejection during cell transplantation therapy.

The programmed cell death 1 ligand 1 (*PD-L1*) gene encodes programmed cell death ligand 1, which, combined with programmed cell death receptor-1, can transmit inhibitory signals, reduce the activation and proliferation of T cells, and inhibit the killing effect after the activation of NK cells. Overexpression of PD-L1 can enhance the immunosuppressive function of cells [12]. At present, the effects of *B2M* gene knockout and *PD-L1* gene overexpression (double gene editing) on the immunogenicity and antigraft rejection ability of allogeneic MSCs after their differentiation have not been reported. The necessity of double gene editing and its advantages over single gene editing may be among the ideal ways to solve the problem of graft rejection in cell transplantation therapy.

Therefore, in this study, canine adipose-derived mesenchymal stem cells (ADSCs) were used as seed cells. By using CRISPR-Cas9 HDR-mediated gene editing technology, the *B2M* gene was knocked out in conjunction with the overexpression of the *PD-L1* gene to explore whether safe gene-edited ADSCs (GeADSCs) with biological characteristics that are not different from those of normal canine ADSCs can be obtained. The immunogenicity and immune escape ability of the strains were tested, and the necessity and advantages of double gene editing were clarified.

Then, on the basis of the obtained GeADSCs, we optimized the previous 6-gene highly regulated gene combination induction program and introduced the 3D cell culture mode. The biological characteristics of the obtained new islet β cells with low immunogenicity were examined via single-cell sequencing, and the induction differentiation efficiency was further improved. Moreover, the method of cell transplantation was optimized, and tissue engineering materials were introduced to investigate the immunogenic changes, therapeutic effects and antigraft rejection ability of newly isolated islet β cells with low immunogenicity.

Finally, this study provides a new method to prolong the survival and functional time of the cells in the transplant recipient and significantly improve the clinical therapeutic effect. To provide a theoretical and technical reference for solving the problem of graft rejection in allogeneic MSCs or after their differentiation and transplantation to treat related diseases. This study provides a new method for the treatment of insulin-dependent diabetes via cell transplantation.

Methods

Gene editing of ADSCs

Using the *B2M* gene of canine ADSCs (GeneID: 100,855,741) as a target gene, 8 sgRNAs were designed and prepared according to the instructions of the Guide-it sgRNA In Vitro Transcription Kit (Takara, 632,635, Japan). The rapid purification of the sgRNAs was performed via the Guide-it IVT RNA Clean-Up Kit (Takara, 632,638, Japan) according to the Guide-it sgRNA Screening Kit (Takara, 632,639, Japan). The efficiency of the sgRNAs was tested, and the optimal sgRNA combination was obtained. The PD-L1 gene of canine ADSCs (GeneID:484,186) was used as the target gene, the SV40T gene and PuroR gene were added, and the dsDNA initiation template was prepared by Wuhan GeneCreate Biological Engineering Co., Ltd., China. A Guided Long ssDNA Production System (Takara, 632,666, Japan) was then used to prepare ssDNA for gene knock-in. Each template could be used to prepare 2 ssDNAs (sense chain and antisense chain), and the purified ssDNA was used for the gene knock-in test.

The third-generation canine ADSCs frozen in the laboratory [5, 6] were resuscitated. The selected sgRNA combination was incubated with TrueCut™ Cas9 protein v2 (Thermo Fisher Scientific, A36499, USA) to prepare the RNP complex. Lipofectamine CRISPRMAX Cas9 transfection reagent (Thermo Fisher Scientific, CMAX00003, USA) was used to transfer RNP complexes into canine ADSCs. ssDNA sense and antisense chains were transferred into canine ADSCs via Advanced DNA RNA Transfection Reagent (Zeta Life, AD601000, USA). SCR7 (Med Chem Express, HY-12742, USA) was added to the cell culture system and cultured for 48–72 h, and Puromycin (Med Chem Express, HY-B1743A, USA) was added to screen the cells.

The efficiency of gene editing was tested by sequencing. A guided-it Knockin Screening Kit (Takara, 632,659, Japan) was used to detect the gene knock-in efficiency of the selected cells. The mRNA expression of the *B2M* gene and *PD-L1* gene was detected via RT–qPCR [34]. The protein expression levels of B2M and PD-L1 were

detected via Western blotting and immunofluorescence staining [16].

GeADSC detection

A Cell Counting Kit-8 (Med Chem Express, HY-K0301, USA) was used to detect the proliferation ability of the obtained cells. Cytokine secretion by the obtained cells (TSG-6, PGE2, HGF, IGF-1, IL-10, VEGF, SDF-1, bFGF, and BDNF) was detected via ELISA kits (Nanjing Jiancheng Biology Engineering Institute, H374-1, H099-1–1, H181, H659-1–1, H009-1–1, H044-1, H201, H039, H069-1–1, China). The obtained cells were evaluated with the corresponding differentiation induction media (Cyagen Biosciences, GUXMX-90021, GUXMX-90041, and GUXMX-90031; China) for their multifunctional differentiation potential (osteogenic, lipogenic and chondrogenic). Immunogenicity testing of the cells was performed, including detection of the expression of MHC-I, MHC-II and costimulatory molecules CD40 and CD80, the proliferation ability of peripheral blood monocytes stimulated by GeADSCs [32], the cytotoxicity of presensitized spleen cells to GeADSCs and the proportion of immune cells in the spleen [40], the peritoneal inflammatory infiltration test to detect the in vivo immune response induced by GeADSCs [6], and the effects of GeADSCs on INF-γ in serum. The cells were labeled with a DiI red fluorescent probe (Beyotime Biotechnology, C1036, China). A total of 10^4 canine GeADSCs were inoculated subcutaneously on both sides of the spine of the dogs, and tumor growth and other adverse reactions were observed. Samples were taken on the 30, 60, 90 and 120th days, and the existence of transplanted cells was observed via fluorescence microscopy (Olympus, BX41, Japan).

Low-immunogenicity new islet β cells

Further optimization of the laboratory's previous program for the differentiation of canine ADSCs into new islet β-cells was performed via a highly effective regulatory gene combination of 6 genes [6]. Normally cultured canine GeADSCs in Nunc™ EasYDish™ (Thermo Fisher Scientific, 150,464, USA) were treated with laboratory-preserved pAdEasy-Pbx1-Pdx1-Ngn3-Pax4 virus particles (MOI = 100) when the cell density reached 70%. After 24 h, the infection efficiency was detected, normal culture medium (α-MEM culture medium containing 10% fetal bovine serum, 1% 100 × Penicillin Streptomycin Solution and 0.25% Anti-Myc Mycoplasma scavenging agent) was used, and the cells were passaged at a ratio of 1:3 every 2 days. Five days after initial infection, the cells were infected at an MOI of 100 via laboratory-preserved pAdEasy-Rfx3-MafA virus particles. The infection efficiency was measured 24 h later, normal culture medium was used, and 2 days after the second infection, the cells were passaged 1:3 and transferred to a Nunclon Sphera 3D culture system (Thermo Fisher Scientific, 174,932, USA) for culture. At the same time, induction culture-1 (high-glucose DMEM culture medium containing 10% Fetal Bovine Serum, 1% 100 × Penicillin Streptomycin Solution and 0.25% Anti-Myc Mycoplasma Scavenging Reagent, 1:200 ITS-X, 650 ng/mL T3, 3 μg/mL Alk5i II, and 10 μg/mL Heparin) was used for 6 days, and the medium was changed every 2 days. At the same time, induction culture-2 (high-glucose culture medium containing 10% Fetal Bovine Serum, 1% 100 × Penicillin Streptomycin Solution and 0.25% Anti-Myc Mycoplasma Scavenging Reagent, 1:200 ITS-X, 650 ng/mL T3, 3 μg/mL Alk5i II, 160 μg/mL N-acetyl Cysteine, 2.5 μg/mL Trolox, and 10 μg/mL Heparin) was used for 6 days, and the medium was changed every 2 days. Normal high-glucose DMEM (high-glucose DMEM culture medium containing 10% fetal bovine serum, 1% 100 × Penicillin Streptomycin Solution and 0.25% Anti-Myc Mycoplasma Scavenging Reagent) was added for 6 days, and the medium was changed every 2 days. New islet β cells with low immunogenicity were obtained.

Detection of low-immunogenicity new islet β cells

The amount of insulin secreted by the cells was measured by repeated stimulation with high glucose (25 mM), low glucose (5 mM) and low glucose (5 mM) + KCl (30 mM) to determine the tolerance of the cells [24]. The new islet β cells were dispersed into single cells, and the cells were subjected to immunofluorescence with primary antibodies (Insulin, NKX6.1, MAFA, PAX4, NGN3, PDX1, NKX2.2, B2M, MHC-I, PD-L1), (Abcam, ab6995, ab221549, ab84987, ab239356, ab216885, ab240318, ab228415, ab215889, England), (Epdi Bioengineering, IPD-ANM2501, China) and corresponding secondary antibodies (Abcam, ab150113, ab150079, England). The ultrastructures of the cells and Insulin, NKX6.1, MAFA, PAX4, NGN3, PDX1 and NKX2.2 particles were detected via electron microscopy (Carl Zeiss AG, Germany) and immunocytolloidal gold labeling techniques.

Single-cell sequencing analysis was performed on new islet β cells, and the original data were filtered and compared with genome data, transcript quantification, and cell identification via Cell Ranger (https://support.10xgenomics.com/single-cell-gene-expression/software/overview/welcome), the official analysis software 10 × Genomics, and finally, the gene expression matrix of each cell was obtained. After filtration through Seurat, the filtration criteria were as follows: number of genes expressed per cell > 500 and mitochondrial genes expressed in < 25% of the cells [3]. With Seurat software, the built-in parameter normalization data are used, the variable features are

identified, the data are normalized, and the highly variable genes are searched [17]. According to gene expression information, cells were classified into multiple clusters via the UMAP algorithm, and the expression of marker genes in each cluster was subsequently checked. The marker genes were selected on the basis of the following criteria: expression in more than 10% of the cells in each cluster, P value ≤ 0.01, and gene expression ploidy logFC ≥ 0.26 [7]. At the same time, Garnett software and the SingleR annotation package were combined to identify cell clusters [17]. Statistical analysis, GO function analysis, KEGG enrichment analysis and protein interaction network analysis were performed on the differentially expressed genes of each cell cluster to study the differences in transcriptional regulation among different cell clusters and explore the differentiation map [19]. Moreover, the immunogenicity of the new islet β cells was tested according to a previously described method.

Treatment of diabetic dogs with low-immunogenicity new islet β cells

All of the dogs were reared, obtained, and housed in accordance with our institute's laboratory animal requirements. All procedures and the study design were conducted in accordance with the Guide for the Care and Use of Laboratory Animals (Ministry of Science and Technology of China, 2006) and were approved by the Animal Ethical and Welfare Committee of Northwest Agriculture and Forest University. The work has been reported in line with the ARRIVE guidelines 2.0.

Dogs (adult beagle dogs) were used as an animal model to establish a canine diabetes model [6] by combining 85% pancreatic resection with 5 mg/kg streptozotocin solution (injected into the superior duodenal artery). The experimental dogs were injected intravenously with propofol (3 ~ 6 mg/kg) (Xi 'an Libon Pharmaceutical Co., Ltd., China) to induce anesthesia before surgery, endotracheal intubation was performed to protect the airway, and a respiratory anesthesia machine was connected. The isoflurane (Shenzhen Reward Life Technology Co., Ltd., China) and oxygen flows were adjusted, and when anesthesia was stably maintained. The operation was subsequently carried out in strict accordance with the established surgical protocol and aseptic rules. During the operation, the central nervous system, cardiovascular system and respiratory system were monitored, and temperature changes were recorded to monitor the animal's status. The dogs were administered Vectaxib chewable tablets (Orbiepharm, China, 3 mg/kg/d, for 5 days) and Beylide (Bayer, Germany, 2.5 mg/kg/d, for 5 days) beginning on the first postoperative day.

Cell transplantation was carried out to treat dog diabetes mellitus, and the transplantation site was selected on the basis of the subcutaneous adipose tissue inside the root of the thigh of the dog. Thirty days before cell transplantation, the fibroin/collagen scaffold [11] was implanted into the transplantation site to obtain a vascularization pouch and shorten the cell colonization time. The cells were labeled with DiI red fluorescent probes, and the cells were divided into 3 groups. Experimental Group 1 ($n=6$): New islet β cells derived from canine GeADSCs (10^6 cells/kg) + canine GeADSCs (10^6 cells/kg) were injected into a vascularization pouch. Experimental Group 2 ($n=6$): New islet β cells derived from canine normal ADSCs (10^6 cells/kg) + canine normal ADSCs (10^6 cells/kg) were injected into a vascularization pouch. In the control group (n = 3), normal saline (1 mL) was injected into the vascularization pouch.

Blood glucose levels were measured every 5 days after transplantation, and glucose tolerance tests were performed when blood glucose levels stabilized [13]. At the same time, one dog in each group was randomly selected to sample the transplant site, and insulin immunofluorescence staining and fluorescence microscopy were performed to determine the survival status and insulin expression of the transplanted cells. On the 80th day, one dog in each group was randomly selected for sample collection from the transplant site, and the infiltration and distribution of immune cells (B cells, T cells, NK cells and macrophages) at the transplant site were detected. Moreover, ELISA (Nanjing Jiancheng Biology Engineering Institute, H002-1–2, H003-1–1, H004, H005-1–2, H007-1–1, H052-1–1, H059, China) was used to detect the contents of related cytokines (IL-1, IL-2, IL-3, IL-4, IL-6, TNF, M-CSF) at the transplantation site. The experimental dogs were euthanized with propofol (20 mg/kg) (Xi 'an Libon Pharmaceutical Co., Ltd., China).

Results

Results of gene editing of ADSCs

In this study, a Guide-it sgRNA In Vitro Transcription Kit was used to obtain 8 sgRNAs (Fig. 1A) by designing 8 upstream primers (Supplementary Document 1). After the sgRNAs were purified, the Guided-it sgRNA Screening Kit is used to detect the editing efficiency of the 8 sgRNAs. Multiple detection results revealed that sgRNAs 3 and 7 had better editing efficiency. In this study, sgRNAs 3 and 7 were used for subsequent experiments (Fig. 1B). The dsDNA initiation template was made via whole gene synthesis (Supplementary document 2). Two ssDNA chains (sense chain and antisense chain) for gene knock-in were prepared through the Guide-it Long ssDNA Production System (Fig. 1C).

sgRNAs numbered 3 and 7 were incubated with Cas9 protein to prepare RNP complexes, which were

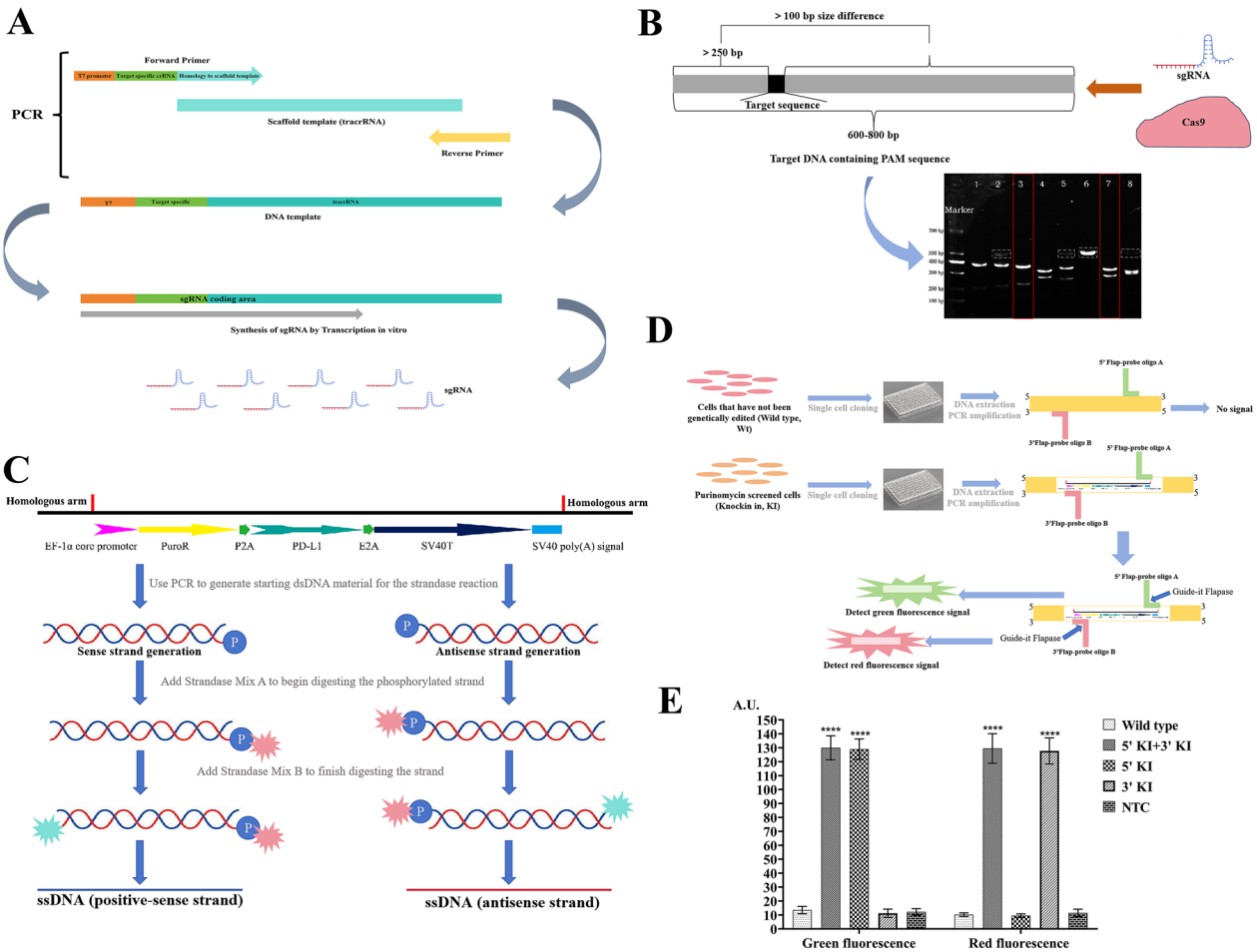

Fig. 1 The Result of gene editing ADSCs. **A**. sgRNAs acquisition process. Guide-it sgRNA In Vitro Transcription Kit was used to obtain 8 sgRNAs. sgRNAs were synthesized by transcription in vitro. **B**. The editing efficiency of 8 sgRNAs. The Guided-it sgRNA Screening Kit is used to detect the editing efficiency of 8 sgRNAs. sgRNAs 3 and 7 have better editing efficiency. Full-length blots/gels are presented in Supplementary document—Uncropped images. **C**. ssDNA acquisition process. dsDNA was obtained by gene synthesis, two ssDNA chains (positive-sense chain and antisense chain) for gene knock-in were prepared through the Guide-it Long ssDNA Production System. D and E. Gene knock-in detection. **D**. The Guide-it Knockin Screening Kit was used for gene knock-in detection. When the gene is successfully knocked in, red and green fluorescence signals are detected. **E**. Both red and green fluorescence signals could be detected in gene knock-in strains, and the red and green fluorescence signals were significantly greater than those in wild strains. ****, $P < 0.0001$

subsequently transferred to canine allogeneic ADSCs. Moreover, the sense and antisense chains of ssDNA were transferred to the above cells, SCR7 was added to the cell culture system, and the cells were cultured for 48 h. The cells were screened with Purinomycin. The cells were cloned and cultured for single-cell proliferation. The Guide-it Knockin Screening Kit was used for gene knockin detection (Fig. 1D, Supplementary document 3). Fluorescence detection revealed that red and green fluorescence was detected in 19 of the 60 cell clones (Fig. 1E). The 19 cells were cloned and inserted into a cluster and cultured, the target sequence of the obtained cells was sequenced, and the sequencing results were correct (Supplementary document 4). The obtained cells were named GeADSCs. The mRNA expression levels of the *B2M* gene and *PD-L1* gene in GeADSCs were detected by RT–qPCR (Supplementary document 5). In GeADSCs, the mRNA expression of the *B2M* gene was extremely significantly lower than that in ADSCs ($P < 0.0001$), and the mRNA expression of the *PD-L1* gene was extremely significantly greater than that in ADSCs ($P < 0.0001$) (Fig. 2A). The protein expression levels of B2M and PD-L1 in the cells were detected by Western blot analysis. In GeADSCs, the B2M protein was not expressed, and the PD-L1 protein was highly expressed; however, in ADSCs, the B2M protein was expressed, but the PD-L1 protein was not highly expressed (Fig. 2B).

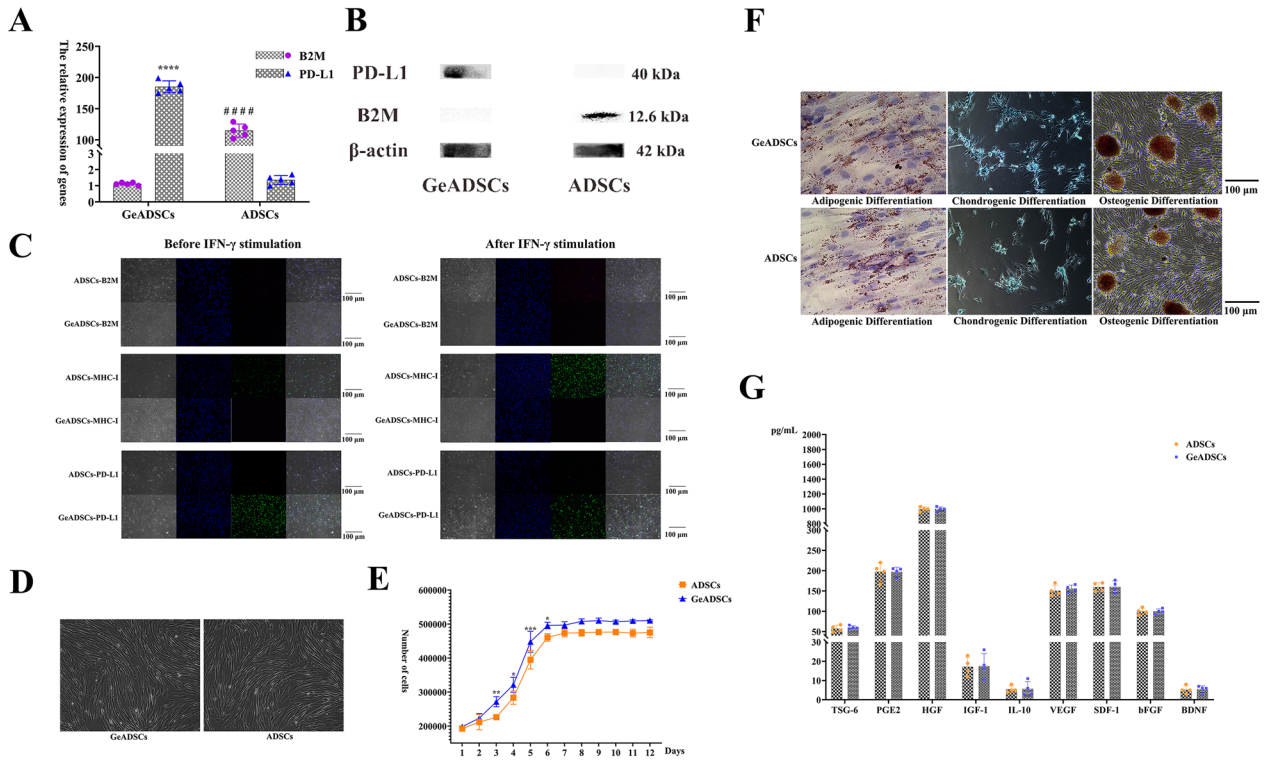

Fig. 2 Biological characteristics of GeADSCs. **A**. The relative expression of genes. In GeADSCs, the mRNA expression of *B2M* gene was extremely significantly lower than that of ADSCs, and the mRNA expression of *PD-L1* gene was extremely significantly higher than that of ADSCs. ****, ####, $P < 0.0001$. **B**. Protein expression detection. In GeADSCs, B2M protein was not expressed and PD-L1 protein was highly expressed, while in ADSCs, B2M protein was highly expressed but PD-L1 protein was not expressed. Full-length blots/gels are presented in Supplementary document—Uncropped images. **C**. B2M, MHC-I and PD-L1 detection. In GeADSCs, the expression of B2M and MHC-I molecules was not detected, PD-L1 is highly expressed before and after IFN-γ stimulation. ADSCs can express B2M and MHC-I molecules, and after stimulation with IFN-γ, the expression of B2M and MHC-I molecules is enhanced. In ADSCs, PD-L1 is not expressed before IFN-γ stimulation, but IFN-γ stimulation can promote the weak expression of PD-L1. The red fluorescence is B2M and the green fluorescence is MHC-I or PD-L1. **D**. Morphological characteristics detection. The morphological characteristics of GeADSCs showed no difference from those of ADSCs. **E**. Cell growth curve. The growth rate of GeADSCs was significantly higher than that of ADSCs, especially on the 3rd, 4, 5 and 6th day. *, $P < 0.05$; **, $P < 0.01$; ***, $P < 0.001$. **F**. Multidirectional differentiation detection. The differentiation performance of GeADSCs was not different from that of ADSCs. **G** The detection of related cytokines. In GeADSCs and ADSCs, there was no difference in the secretion of various cytokines

The expression of B2M and MHC-I molecules was not detected by immunofluorescence before or after GeADSCs were stimulated with IFN-γ. Before stimulation with IFN-γ, ADSCs can express B2M and MHC-I molecules, and after stimulation with IFN-γ, the expression of B2M and MHC-I molecules is increased. In GeADSCs, PD-L1 is highly expressed before and after IFN-γ stimulation. In ADSCs, PD-L1 is not expressed before IFN-γ stimulation, but IFN-γ stimulation can promote weak expression of the PD-L1 protein (Fig. 2C).

The GeADSCs obtained in this study did not express the B2M protein (MHC-I molecules) but overexpressed the PD-L1 protein and successfully achieved gene editing in ADSCs.

Biological characterization of GeADSCs

Under the same culture conditions, the morphological characteristics of GeADSCs showed no difference from those of ADSCs, with long spindle shapes and adherent growth (Fig. 2D). The growth rate of GeADSCs was significantly greater than that of ADSCs, especially on the 3rd, 4, 5 and 6th days ($P < 0.05$) (Fig. 2E). With respect to multidirectional differentiation, the differentiation performance of GeADSCs was not different from that of ADSCs, and all of them could differentiate into adipose, cartilage or bone cells (Fig. 2F). In the detection of related cytokines, under the same culture conditions, there was no difference in the secretion of various cytokines, and related immune regulatory factors and growth factors could be secreted (Fig. 2G). The biological characteristics of GeADSCs were not affected by gene editing.

Immunogenicity test results of GeADSCs

After GeADSCs were obtained, their immunogenicity was detected. First, the immunophenotype of the cells was detected. In GeADSCs and ADSCs, the expression of MHC-II molecules and the costimulatory molecules CD40 and CD80 was very low, and there was no significant difference. In ADSCs, MHC-I molecules were highly expressed, which was significantly greater than that in GeADSCs ($P < 0.0001$) (Fig. 3A). In terms of the proliferation ability of peripheral blood monocytes stimulated with GeADSCs and ADSCs, there was no significant difference in the immunosuppressive ability of GeADSCs and ADSCs. As the number of peripheral monocytes increased, the stimulation index increased; that is, the proliferation ability of peripheral monocytes increased, but both were lower than that of the peripheral blood monocyte group. These results indicate that both GeADSCs and ADSCs can inhibit the proliferation of peripheral blood monocytes (Fig. 3B). After the intracavitary injection of GeADSCs and ADSCs, the cells in the spleen were examined. After the intraperitoneal injection of GeADSCs, the number of CD4 + T cells in the spleen was significantly lower than that in the ADSC group ($P < 0.0001$). There was no significant difference in CD8 + T cells between the GeADSC and ADSC groups (Fig. 3C). After the intraperitoneal injection of GeADSCs, the number of CD19 + B cells in the spleen decreased, which was significantly lower than that in the ADSC group ($P < 0.0001$) (Fig. 3D). For CD + Foxp3 + Treg cells, there was no significant difference between the GeADSC and ADSC groups (Fig. 3E). Subsequently, spleen cells were cocultured with GeADSCs or ADSCs, and it was found that spleen cells could cause the apoptosis of both GeADSCs and ADSCs in a dose-dependent manner. As the proportion of spleen cells increased, the percentage of apoptotic cells increased, but the percentage of apoptotic GeADSCs was significantly lower than that of the ADSC group ($P < 0.0001$) (Fig. 3F). After the intraperitoneal injection of GeADSCs, the number of CD45 + and CD3e + cells in the abdominal cavity was significantly lower than that in the ADSC group ($P < 0.0001$) (Fig. 3G). After the intraperitoneal injection of GeADSCs and ADSCs, the serum IFN-γ concentration was detected, and the level in the GeADSC group was significantly lower than that in the ADSC group ($P < 0.0001$) (Fig. 3H). Compared with that of ADSCs, the immunogenicity of GeADSCs was significantly reduced.

To further test the survival time of GeADSCs after transplantation in vivo, DiI red fluorescent probes were used to label the cells, and the cells were inoculated subcutaneously on both sides of the spines of the dogs. After the cells were inoculated, there were no adverse reactions, such as tumors, at the inoculated site. Samples were taken on the 30, 60, 90 and 120th days, and the status of the transplanted cells was detected. The number of implanted cells decreased over time (Fig. 3I), and at Days 60, 90, and 120, the number of cells present in the ADSC group was significantly lower than that in the GeADSC group (Fig. 3J) ($P < 0.0001$). The immunogenicity of GeADSCs is reduced, which can resist transplant rejection to a certain extent and prolong the time in vivo after transplantation.

(See figure on next page.)

Fig. 3 Immunogenicity detection results. **A**. The immunophenotype detection of the cells. In GeADSCs, ADSCs, GeADSCs-RM-βCs and ADSCs-RM-βCs, the expressions of MHC-II molecules and CD40 and CD80 were very low, and there was no significant difference. In ADSCs and ADSCs-RM-βCs, MHC-I molecule showed high expression, which was significantly higher than GeADSCs and GeADSCs-RM-βCs. ****, ####, $P < 0.0001$. **B**. The proliferation ability of peripheral blood monocytes. There was no significant difference in the immunosuppressive ability of GeADSCs and ADSCs. GeADSCs and ADSCs can inhibit the proliferation of peripheral blood monocytes. the immunosuppressive ability of the ADSCs-RM-βCs and GeADSCs-RM-βCs was significantly lower than that of GeADSCs and ADSCs. ****, $P < 0.0001$. **C**. Spleen cells detection. In GeADSC group, $CD4^+$ T cells were significantly lower than those in the ADSC group. ****, $P < 0.0001$. In GeADSC-RM-βC group, $CD4^+$ T cells were significantly lower than those in the ADSC-RM-βC group. ####, $P < 0.0001$. For $CD8^+$ T cells, there was no significant difference between the GeADSC and ADSC groups. In GeADSC-RM-βC group, $CD8^+$ T cells were significantly lower than those in the ADSC-RM-βC group. ****, $P < 0.0001$. **D**. $CD19^+$ B-cells detection. In GeADSC group, $CD19^+$ B-cells were decreased, which was significantly lower than that in ADSC group. ****, $P < 0.0001$. In GeADSC-RM-βC group, $CD19^+$ B-cells were decreased, which was significantly lower than that in ADSC-RM-βC group. ####, $P < 0.0001$. **E**. CD^+ $Foxp3^+$ Treg cells detection. There was no significant difference between GeADSC, ADSC, GeADSC-RM-βC and ADSC-RM-βC groups. **F**. Apoptosis of GeADSCs and ADSCs. As the proportion of spleen cells increased, the apoptosis rate of cells increased. The apoptosis rate of GeADSCs was significantly lower than that of ADSCs. ****, $P < 0.0001$. The apoptosis rate of GeADSCs-RM-βCs was significantly lower than that of ADSCs-RM-βCs. ####, $P < 0.0001$. **G**. $CD45^+$ and $CD3e^+$ cells detection. The number of $CD45^+$ and $CD3e^+$ cells in GeADSC group was significantly lower than that in the ADSC group. ****, $P < 0.0001$. The number of $CD45^+$ and $CD3e.^+$ cells in GeADSC-RM-βC group was significantly lower than that in the ADSC-RM-βC group. ####, $P < 0.0001$. **H**. IFN-γ detection. After intraperitoneal injection of cells, the GeADSC group was significantly lower than the ADSC group. ****, $P < 0.0001$. The GeADSC-RM-βC group was significantly lower than the ADSC-RM-βC group. ####, $P < 0.0001$. **I**. The survival time of GeADSCs after transplantation in vivo. The number of implanted cells decreased over time. Blue fluorescence indicates the nucleus and red fluorescence indicates the cells. **J**. Cell count detection. The number of cells present in the ADSC group was significantly lower than that in the GeADSC group. ****, ####, ^^^^, $P < 0.0001$

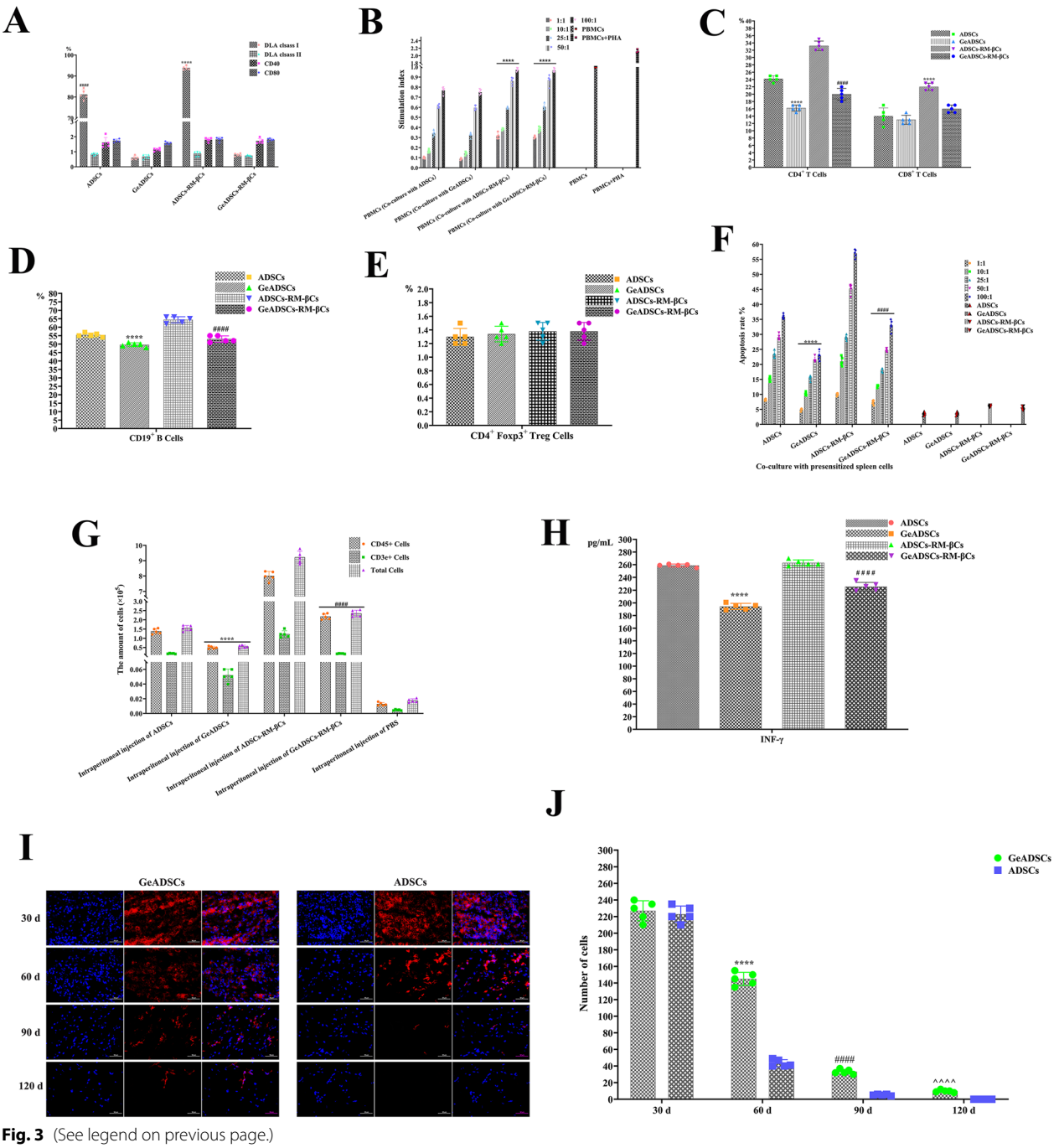

Fig. 3 (See legend on previous page.)

Biological characteristics of newly islet β cells with low immunogenicity

The program for the differentiation of canine ADSCs into new islet β cells induced by the highly efficient regulatory gene combination of 6 genes in the laboratory was further optimized. We induced the differentiation of GeADSCs and obtained new islet β cells (RM-βCs), and the obtained cells were round and suspended in cell culture medium (Fig. 4A). By repeated stimulation with high glucose (25 mM), low glucose (5 mM) and low glucose (5 mM) + KCl (30 mM), the insulin secretion of the cells was measured. RM-βCs respond to continuous glucose stimulation, and insulin secretion can reach more than 60% of that of mature islet cells regardless of the presence of low glucose or high glucose. This value was significantly greater than that of canine ADSCs ($P < 0.0001$)

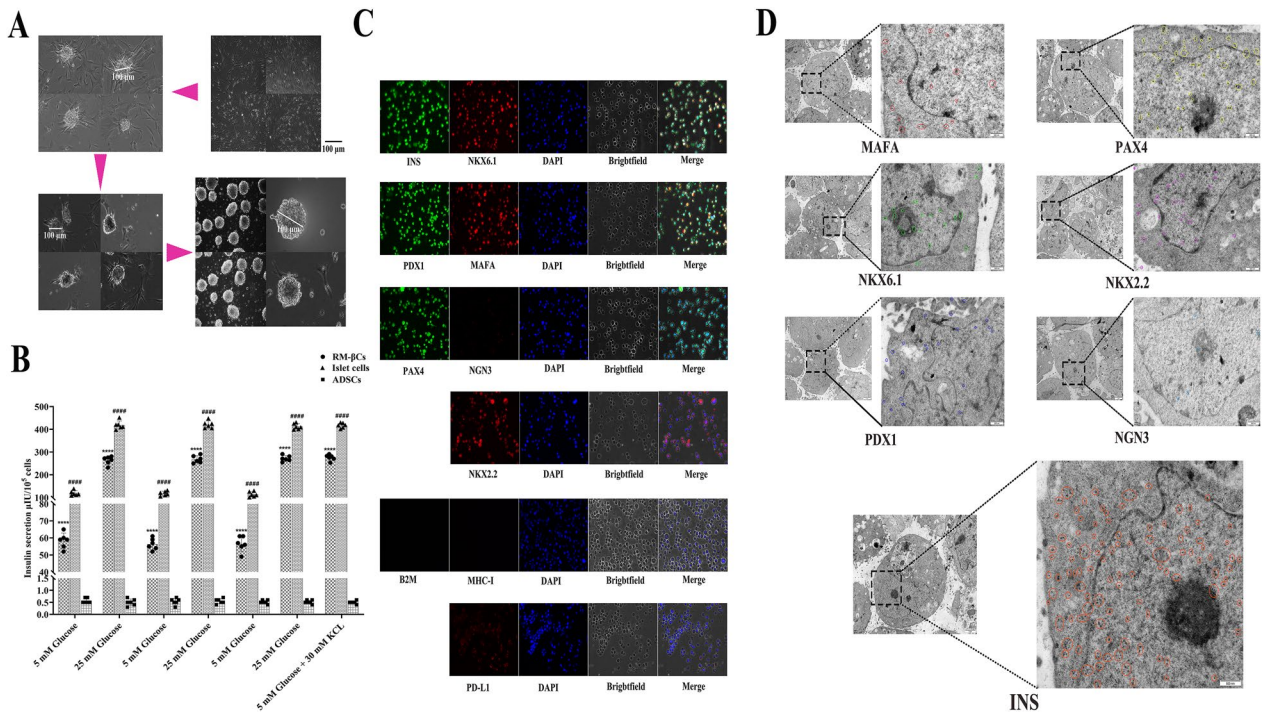

Fig. 4 Biological characteristics of low immunogenic new islet β cells. **A**. The differentiation of canine ADSCs into new islet β cells. The obtained new islet β cells (RM-βCs) were round and suspended in cell culture medium. **B**. The insulin secretion of the cells. RM-βCs could respond to continuous glucose stimulation, and insulin secretion could reach more than 60% of mature islet β cells in low glucose or high glucose. Significantly higher than canine ADSCs. ****, $P < 0.0001$. #### indicated that RM-βC and ADSC groups were significantly lower than mature islet β cells group ($P < 0.0001$). **C**. Immunofluorescence staining detection. Insulin, NKX6.1, PDX1, MAFA, PAX4, NKX2.2 and PD-L1 showed high expression, NGN3 showed weak expression, and B2M and MHC-I were not expressed. **D**. Electron microscopy detection. For NKX6.1, PDX1, MAFA, PAX4 and NKX2.2, related particles were detected in the cells, NGN3 particles were almost undetected, and Insulin particles were detected in large numbers. Different colored circles represent the corresponding particles

(Fig. 4B). The RM-βCs were dispersed into single cells, and immunofluorescence staining was performed on the cells with related antibodies. Insulin, NKX6.1, PDX1, MAFA, PAX4, NKX2.2 and PD-L1 were expressed at high levels, NGN3 was weakly expressed, and B2M and MHC-I were not expressed (Fig. 4C). The ultrastructures of the cells were detected via electron microscopy and immunocolloidal gold labeling techniques. For NKX6.1, PDX1, MAFA, PAX4 and NKX2.2, related particles were detected in the cells, NGN3 particles were almost undetected, and Insulin particles were detected in large numbers (Fig. 4D). The RM-βCs obtained in this study had the characteristics of islet β cells.

Single-cell sequencing of new islet β cells with low immunogenicity

In this study, 7530 new islet β cells (RM-βCs) were sequenced via single-cell analysis. The data discussed in this publication have been deposited in NCBI's Gene Expression Omnibus (Edgar et al., 2002) and are accessible through GEO series accession number accession number GSE267867 (https://www.ncbi.nlm.nih.gov/geo/query/acc.cgi?acc=GSExxx). Genome comparison, background cell filtering and UMI counting of transcripts were performed on the original sequencing data via Cell Ranger. A gene–barcode matrix was generated via a cell barcode, sample clustering and gene expression analysis were subsequently performed, and the statistical results of the sequencing data were output (Supplementary document 6). The expression levels of the genes detected in each cell were calculated according to Barcode, UMI and other information (Supplementary document 7). For filtering by Seurat, see Supplementary document 8 for the statistical table of cell filtration and Supplementary document 9 for the distribution of basic information of each sample cell before cell filtration. For the distribution of basic information for each sample cell after cell filtration, see Supplementary document 10.

The cells were subdivided into 13 cell clusters according to their gene expression patterns. The number of cells in each cluster is shown in Supplementary Document 11, and the percentage statistics are shown in Supplementary Document 12. After the end of the clustering, these cells were visualized via the UMAP algorithm (Fig. 5A),

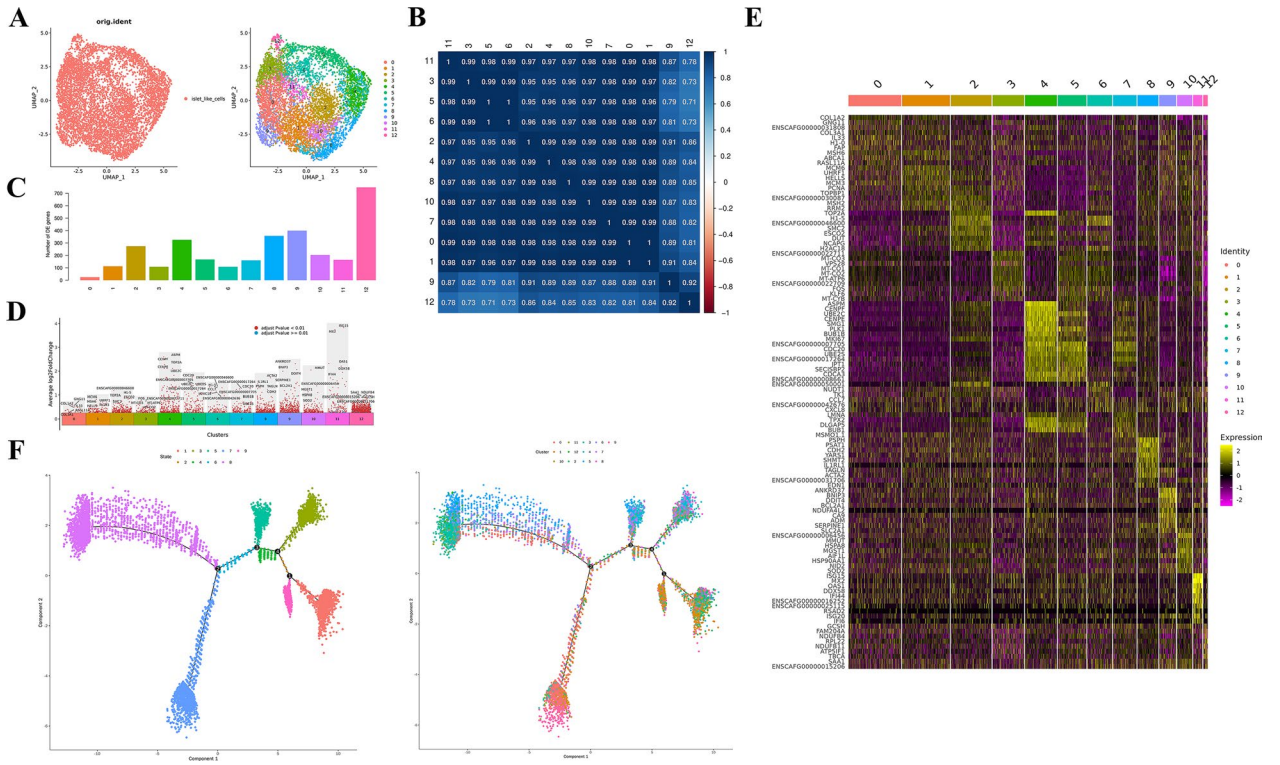

Fig. 5 Single cell sequencing of low immunogenic new islet β cells. **A**. The cells were visualized, it was divided into 13 clusters. Each dot represents a cell. Left: Different colors represent different samples of cells; Right: Different colors indicate different clusters of cells. **B**. The correlation heat map. The cluster 9 and 12 were highly correlated, and the other numbered cluster were highly correlated. **C**. The output standard of Marker genes. The number of differentially up-regulated genes in clusters 9 and 12 was the highest, with 399 and 748 genes respectively. **D**. The volcano map of Marker genes. The dots in the figure are differentially upregulated genes, showing by default the top 5 genes of each cell population by their differentially multiples, and the horizontal axis shows the proportion of the gene expressed in the target cell population—the proportion of the gene expressed in other cell populations. **E**. The heat map of Marker gene expression. Rows represent genes, characters on the left represent gene names, columns represent individual cells, and characters on the top represent cell subpopulation numbers. Colors from purple to black to yellow represent gene expression levels from low to high. TOP10 genes of each cluster Marker are selected for genes. **F**. The development and evolution process of cells. There were 4 biological process decision points in 13 clusters (6482 cells)

and a correlation heatmap was drawn by calculating the correlation among each cluster. The clusters numbered 9 and 12 were highly correlated, and the other numbered clusters were highly correlated (Fig. 5B). According to the output standard of the marker gene, the number of marker genes in each cluster was obtained, and a total of 3149 genes were obtained. Among them, the number of differentially upregulated genes in Clusters 9 and 12 was the highest, with 399 and 748 genes, respectively (Fig. 5C). See Supplementary document 13 for detailed information on the marker genes in each cluster and Fig. 5D for the volcano plots of the marker gene differences in different cell clusters. See Supplementary document 14 for the volcano map of marker gene differences and expression ratios in different cell clusters and Fig. 5E for the heatmap of marker gene expression in each cell cluster. The top 10 marker genes in each cell cluster were subsequently identified and plotted via Violin, Umap, bubble and ridge maps (Supplementary Document 15). GO enrichment analysis and KEGG enrichment analysis were subsequently performed for all marker genes (Supplementary document 16). Monocle2 software was used to simulate the development and evolution process of cells through gene expression, and subsequent quasitime series analysis was conducted on 6482 cells. There were 4 biological process decision points in 13 clusters (Fig. 5F).

Finally, the characteristic genes of islet beta cells, islet alpha cells, pancreatic stem cells and duct cells were used to identify the cell types of each cluster. Multiple characteristic genes (*G6PC2*, *GNAS*, *CSDE1*, *HEPACAM2*, *OXLD1*, *APLP2*, *AP3B1*, *ALCAM*, etc.) of islet β cells were highly expressed in each cluster (Fig. 6A). In addition, several cell clusters also expressed characteristic genes of pancreatic stem cells (Fig. 6B) and alpha cells (Fig. 6C), including *LGR5*, *CXCR4*, *ARX*, *GCG*, *IRX2*, and *LOXL4*. Individual clusters also expressed a characteristic gene of conduit cells (*PROM1*) (Fig. 6D).

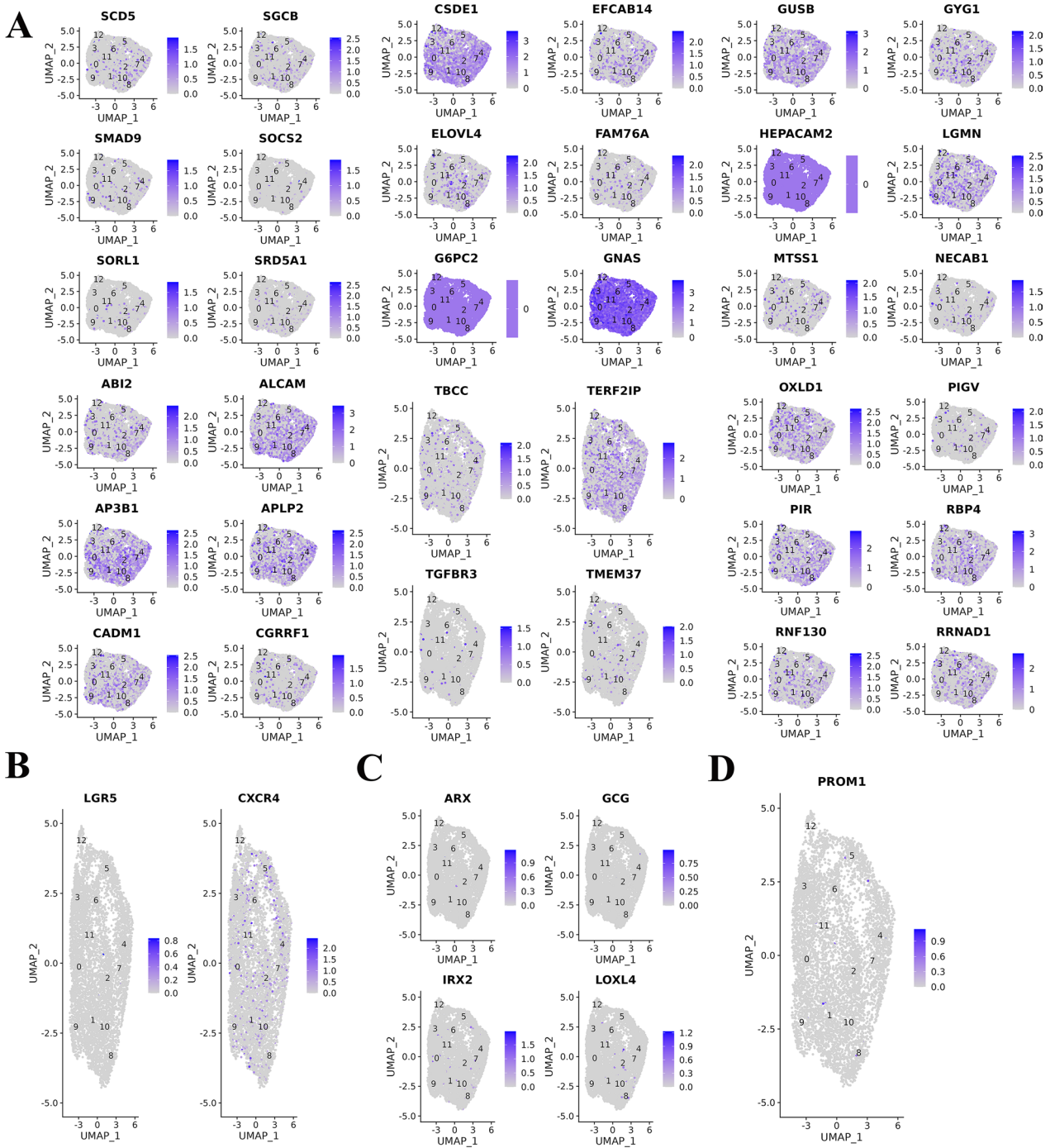

Fig. 6 A. Multiple characteristic genes of mature islet β cells were highly expressed in each cluster. **B**. Several cell clusters expressed characteristic genes of pancreatic stem cells. **C**. Several cell clusters expressed characteristic genes of pancreatic stem cells alpha cells. **D**. Individual clusters expressed a characteristic gene of conduit cells

The RM-βCs obtained in this study have the characteristics of canine islet β cells and can be used for cell transplantation in the treatment of canine diabetes.

Detection of the immunogenicity of new islet β cells

After the immunogenicity of RM-βCs from GeADSCs (GeADSCs-RM-βCs) was detected, RM-βCs from normal ADSCs (ADSCs-RM-βCs) were used as controls.

First, the immunophenotype of the cells was detected. In the ADSCs-RM-βCs, the MHC-I molecule was highly expressed, which was significantly greater than that in the GeADSCs-RM-βCs ($P < 0.0001$). MHC-II molecules and the costimulatory molecules CD40 and CD80 were almost not expressed in the two groups of cells, and there was no significant difference (Fig. 3A). In terms of the proliferation ability of peripheral blood monocytes stimulated with ADSCs-RM-βCs and GeADSCs-RM-βCs, there was no significant difference in immunosuppressive ability between ADSCs-RM-βCs and GeADSCs-RM-βCs. However, the immunosuppressive ability of the ADSCs-RM-βCs and GeADSCs-RM-βCs was significantly lower than that of the GeADSCs and ADSCs ($P < 0.0001$), the stimulation index increased with increasing number of peripheral monocytes, and both the ADSCS-RM-βCs and the GeADSCs-RM-βCs inhibited the proliferation of peripheral monocytes to a certain extent (Fig. 3B). After the intraperitoneal injection of ADSCs-RM-βCs or GeADSCs-RM-βCs, the number of cells in the spleen was detected. After the intraperitoneal injection of GeADSCs-RM-βCs, both the number of CD4 + T cells and the number of CD8 + T cells in the spleen decreased, which was significantly lower than that in the ADSC-RM-βC group ($P < 0.0001$) (Fig. 3C). After the intraperitoneal injection of GeADSCs-RM-βCs, the number of CD19 + B cells in the spleen was significantly lower than that in the ADSC-RM-βC group ($P < 0.0001$) (Fig. 3D). For CD + Foxp3 + Treg cells, there was no significant difference between the ADSC-RM-βC and GeADSC-RM-βC groups (Fig. 3E). Subsequently, spleen cells were cocultured with ADSCs-RM-βCs or GeADSCs-RM-βCs, and the results revealed that spleen cells caused the apoptosis of both ADSCs-RM-βCs and GeADSCs-RM-βCs in a dose-dependent manner. With increasing proportions of spleen cells, the percentage of apoptotic cells increased. The apoptosis rate of GeADSCs-RM-βCs was significantly lower than that of ADSCs-RM-βCs ($P < 0.0001$) (Fig. 3F). After the intraperitoneal injection of GeADSCs-RM-βCs, the number of CD45 + and CD3e + cells in the abdominal cavity decreased and was significantly lower than that in the ADSC-RM-βC group ($P < 0.0001$) (Fig. 3G). After intrabitoneal injection of ADSCs-RM-βCs and GeADSCs-RM-βCs, serum IFN-γ was detected, and the level of IFN-γ in the GeADSC-RM-βC group was significantly lower than that in the ADSC-RM-βC group ($P < 0.0001$) (Fig. 3H).

The immunogenicity of GeADSCs-RM-βCs was significantly lower than that of ADSCS-RM-βCs but was greater than that of GeADSCs and similar to that of ADSCs.

Results of the use of new islet β cells with low immunogenicity in the treatment of canine diabetes mellitus

Cell transplantation was carried out to treat dog diabetes mellitus. The transplantation site was selected in the subcutaneous adipose tissue of the medial thigh root of the dog. The fibroin/collagen scaffold was implanted into the transplantation site 30 days before cell transplantation. After 30 days of stent implantation, some of the scaffold remained at the transplant site, the surrounding tissues grew into the scaffold, and blood vessels could be seen in the scaffold. Implantation of the scaffold resulted in the formation of a vascularized pouch at the transplant site (Fig. 7A), which could provide living space for cells and shorten the time of cell colonization. The DiI red fluorescent probe was subsequently used to label the cells, and the cells were injected into the scaffold at the transplant site. The day of implantation was recorded as Day 0, and the blood glucose levels of the experimental dogs were measured every 5 days. In Experimental Group 1 (GeADSCs-RM-βCs + GeADSCs), the blood glucose level of the dogs decreased below 15 mmol/L on Day 10, stabilized from Day 25, began to rise on Day 215, and rose above 15 mmol/L on Day 230 (Fig. 7B). In Experimental Group 2 (ADSCs-RM-βCs + ADSCs), the blood glucose level of the dogs decreased to less than 15 mmol/L on Day 10, stabilized from Day 25, began to rise on Day 135, and rose to more than 15 mmol/L on Day 155. Insulin (Morning: 4 IU, Evening: 4 IU) was injected from Day 185, and the amount of insulin was adjusted at any time until the blood glucose level became normal and stable (Fig. 7B). In the control group (saline group), the blood glucose level of the dogs continued to rise, insulin was injected on the 120th day (Morning: 5 IU, Evening: 5 IU), and the amount of insulin was adjusted at any time until the blood sugar level became normal and stable (Fig. 7B). In the glucose tolerance experiment, in the GeADSC-RM-βC + GeADSC group and the ADSC-RM-βC + ADSC group, the blood glucose level decreased to near-normal levels after 120 min of glucose injection, whereas in the saline group, the blood glucose level remained high (Fig. 7C). The implanted cells responded to glucose stimulation.

These results indicate that RM-βCs can secrete insulin, play a biological role, respond to glucose stimulation in transplant recipients, and reduce the blood glucose level in diabetic dogs. The time of GeADSCs-RM-βCs + GeADSCs in vivo was significantly longer than that of the ADSC-RM-βCs + ADSCs group, and

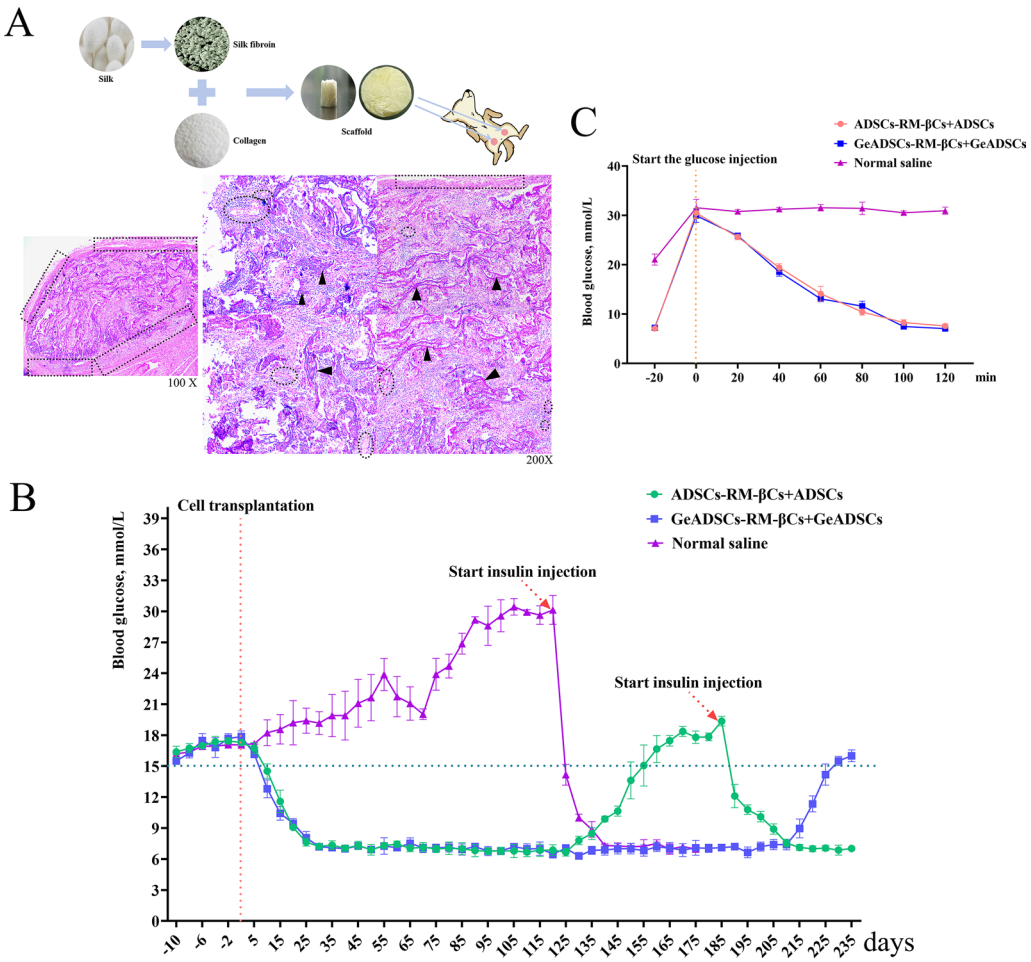

Fig. 7 Low immunogenic new islet β cells treat canine diabetes mellitus. **A**. The fibroin/collagen scaffold was implanted into the transplantation site. After 30 days, there was still a part of the scaffold (as shown by black arrow) at the transplant site, and blood vessels (as shown by black dotted circle) could be seen in the scaffold. Implantation of the scaffold formed a vascularized pouch (as shown by black dotted square) at the transplant site. **B**. The blood glucose of the experimental dogs. In GeADSCs-RM-βCs + GeADSCs group, the blood glucose of dogs dropped below 15 mmol/L on day 10, stabilized from day 25, began to rise on day 215, and rose above 15 mmol/L on day 230. In ADSCs-RM-βCs + ADSCs group, the blood glucose of dogs dropped below 15 mmol/L on day 10, stabilized from day 25, began to rise on day 135, and rose to more than 15 mmol/L on day 155. In saline group, the blood glucose of the dogs continued to rise. **C**. The glucose tolerance experiment. In the GeADSCs-RM-βCs + GeADSCs group and the ADSCs-RM-βCs + ADSCs group, blood glucose dropped to near-normal levels after 120 min of glucose injection, while in the saline group, blood glucose remained high

GeADSCs-RM-βCs and GeADSCs could resist graft rejection to a certain extent.

On the 50th day after cell transplantation, samples were randomly selected from the transplant site. Frozen section examination of the transplant site revealed that there were still residual scaffolds at the transplant site on the 50th day, and many cells gathered between the scaffolds (Fig. 8A). Insulin immunofluorescence staining of the aggregated cells revealed that the aggregated cells in Experimental Group 1 and Experimental Group 2 secreted insulin, whereas no insulin-secreting cells were found in the control group (Fig. 8B). These insulin-secreting cells also express red fluorescence, a marker made with DiI prior to transplantation, demonstrating that the transplanted islet beta cells can express insulin at the transplant site (Fig. 8C). The above results also revealed that the transplanted islet β-cell clusters dispersed into single cells after they entered the body, with only a small number of cell clusters present (Fig. 8D). Moreover, more neovascularization occurred at the transplantation site, the cells around the site of neovascularization were implanted cells, and the implanted cells secreted insulin, which was highly important for the colonization and biological function of the implanted cells (Fig. 8E). In addition, we examined the adipose tissue surrounding the transplant site and found that the implanted cells

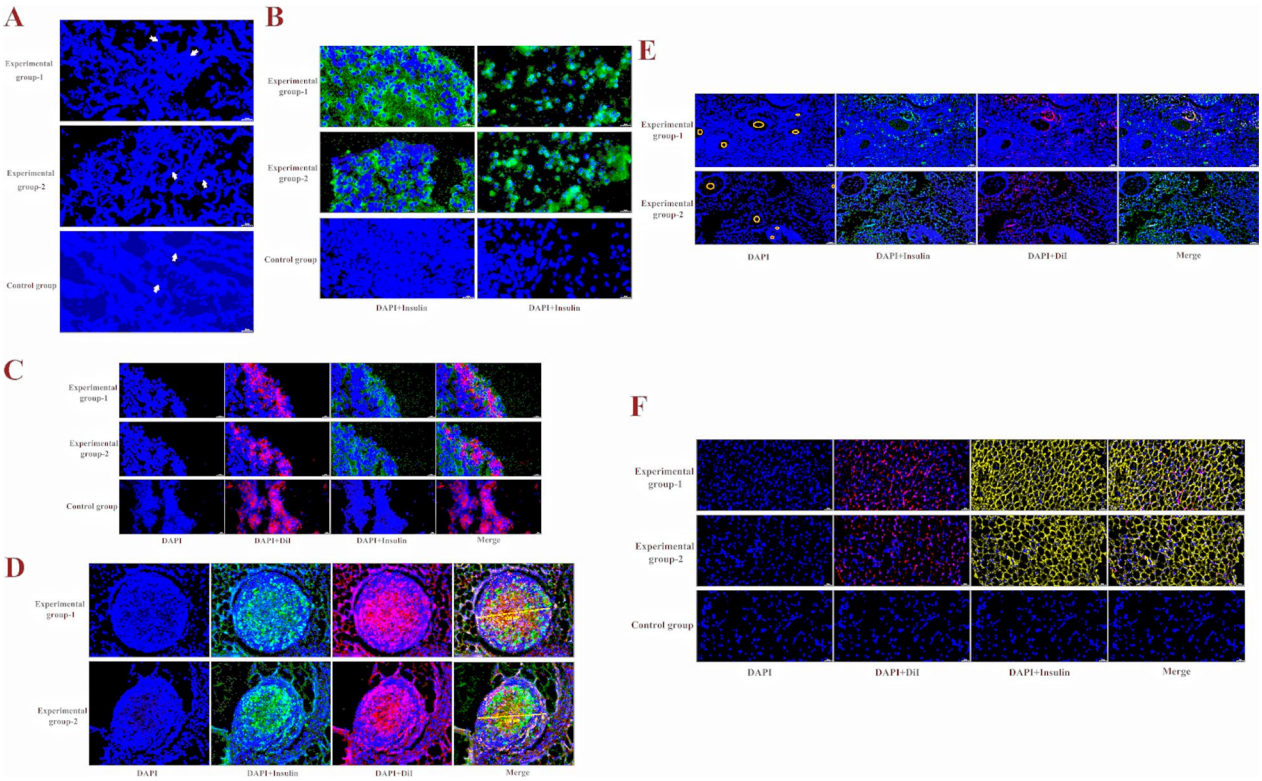

Fig. 8 The results of graft detection. **A**. There were still residual scaffolds in the transplant site on the 50th day, and many cells gathered between the scaffolds. The blue dot is the nucleus, and the white arrow indicates the remnant scaffold. **B**. The aggregated cells in Experimental Group 1 and Experimental Group 2 secreted insulin, while no insulin-secreting cells were found in the control group. Green fluorescence is insulin. **C**. These insulin-secreting cells also express red fluorescence, the transplanted islet β cells can express insulin at the transplant site. **D**. Only a small number of cell clusters present. **E**. The cells around the neovascularization were implanted cells, and the implanted cells secreted insulin. Yellow circles indicate blood vessels. **F**. The implanted cells migrated to the surrounding adipose tissue and secreted insulin was distributed in the adipose tissue

migrated to the surrounding adipose tissue and that secreted insulin was distributed in the adipose tissue, but this was not found in the control group (Fig. 8F). These results indicate that the implanted cells can colonize and migrate to the transplant site and secrete insulin.

Results of antigraft rejection by new islet β cells with low immunogenicity

On the 80th day after cell transplantation, samples were randomly selected from the transplant sites, and the tissues were frozen and subjected to immunofluorescence staining. In Experimental Groups 1 and 2, B-cell aggregation was observed, and the number of B cells in Experimental Group 2 was significantly greater than that in Experimental Group 1 ($P < 0.0001$); however, in the control group, only a very small number of B cells were aggregated, which was significantly lower than that in Experimental Groups 1 and 2 ($P < 0.0001$) (Fig. 9A and F). Moreover, macrophages and NK cells were clustered at the cell transplantation site in Experimental Groups 1 and 2, and the number of macrophages and NK cells in Experimental Group 2 was extremely significantly greater than that in Experimental Group 1 ($P < 0.0001$), whereas the number of NK cells and macrophages in the control group was extremely significantly lower than that in Experimental Groups 1 and 2 ($P < 0.0001$) (Fig. 9B and F). In the helper T-cell assay, there was no significant difference in the number of cells in Experimental Groups 1 and 2, but the number of cells in both groups was significantly greater than that in the control group ($P < 0.0001$) (Fig. 9C and F). The number of cytotoxic T cells in Experimental Group 2 was extremely significantly greater than that in the control group ($P < 0.0001$) and significantly greater than that in Experimental Group 1 ($P < 0.05$), the Experimental Group 1 was significantly greater than that in control group ($P < 0.05$) (Fig. 9D and F). Cytokine detection at the transplantation site revealed that the levels of IL-2, IL-3, IL-4 and IL-6 in Experimental Groups 1 and 2 were not significantly different from those in the control group. However, the levels of IL-1, TNF and M-CSF in Experimental Group

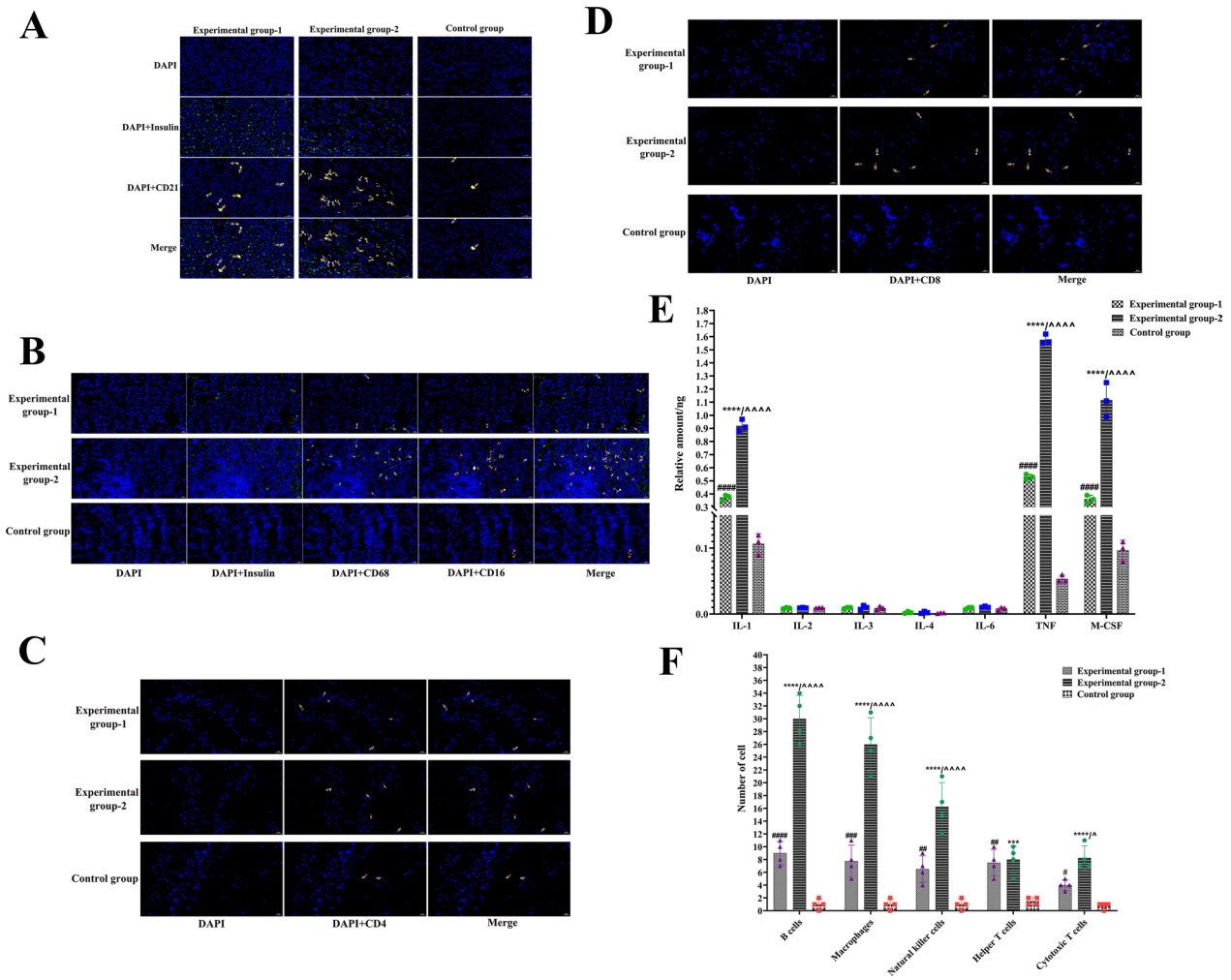

Fig. 9 The results of antigraft rejection of low immunogenic new islet β cells. **A**. In Experimental Groups 1 and 2, B-cell aggregation was observed. CD21 indicates B-cell. **B**. Macrophages and NK cells can be seen clustered at the cell transplantation site in Experimental Groups 1 and 2. CD16 indicates NK cells. CD68 indicates Macrophages cells. **C**. In the helper T cell assay, there was no significant difference in the number of cells in Experimental Groups 1 and 2. CD4 indicates helper T cells. **D**. For cytotoxic T cells, Experimental Group 2 was significantly higher than Experimental Group 1. CD8 indicates cytotoxic T cells. **E**. IL-2, IL-3, IL-4 and IL-6 in Experimental Groups 1 and 2 were not significantly different from those in control group. In the detection of IL-1, TNF and M-CSF, Experimental Group 2 was significantly higher than Experimental Group 1 (****, $P < 0.0001$), and Experimental Groups 1 and 2 were significantly higher than control group (####, ^^^^, $P < 0.0001$). **F**. **** and *** indicates Experimental Group 2 was extremely significantly higher than control group. ####, ###, ## indicates Experimental Group 1 was extremely significantly higher than control group. # indicates Experimental Group 1 was significantly higher than that of control group. ^^^^ indicates Experimental Group 2 was extremely significantly higher than Experimental Group 1. ^ indicates Experimental Group 2 was extremely significantly higher than Experimental Group 1

2 were significantly greater than those in Experimental Group 1 ($P < 0.0001$), and those in Experimental Groups 1 and 2 were significantly greater than those in the control group ($P < 0.0001$) (Fig. 9E).

Although there was transplantation rejection in both Experimental Group 1 and Experimental Group 2, the rate of transplantation rejection in Experimental Group 1 was significantly lower than that in Experimental Group 2, thus prolonging the biological function time of the cells in Experimental Group 1 and significantly improving the clinical therapeutic effect.

Discussion

Halm et al. reported that after CRISPR-Cas9 technology was used to eliminate the expression of MHC-I molecules on the surface of human MSCs, the gene expression, activity, proliferation and in vitro differentiation potential of MSCs were not affected, and the survival rate of

cells after allotransplantation was significantly increased. Eliminating the expression of MHC-I molecules on the cell surface is an effective strategy to prevent the immune rejection of allogeneic MSCs [14]. However, since MHC-I is a ligand of the NK cell-killing inhibitory receptor, the deletion of MHC-I can activate NK cells and kill the allogeneic MSC-B2M knockout strain by NK cells after transplantation in vivo [10]. Gutierrez et al. reported that genetically engineered new islet β cells overexpressing PD-L1 molecules on the cell surface reduced the stimulation of T cells [4]. Therefore, double gene editing was performed in this study; that is, the *B2M* gene was knocked out, and the *PD-L1* gene was overexpressed, with the goal of obtaining allogeneic MSCs with lower immunogenicity. In this study, it was found that allogeneic MSCs have certain immunogenicity, which is significantly enhanced after implantation in vivo, and can stimulate the body to produce transplant rejection. However, after double-gene editing, the biological function of GeADSCs is not affected, and the immunogenicity of GeADSCs is significantly reduced. After transplantation, the survival time of GeADSCs in vivo is significantly longer than that of allogeneic MSCs. The GeADSCs obtained in this study can play biological functions in the body for a longer period of time and help to better repair tissues.

When allogeneic MSCs are differentiated, their immunogenicity is significantly enhanced, and the recipient's immune system can be cleared more quickly after transplantation in vivo, increasing the difficulty of clinical application. When they are applied in tissue engineering or cell transplantation therapy, it is necessary to consider the impact of changes in immunogenicity on the effects of transplantation [30]. In previous studies, we reported that the immunogenicity of canine allogeneic MSCs was significantly greater than that of adipose MSCs after their differentiation into new islet β-cells, and the transplantation of new islet β-cells could cause immune rejection reactions, such as inflammatory cell and immune cell infiltration, which shorten the time for the transplantation of transplanted cells to play a role, resulting in the therapeutic effect not reaching the ideal state [6]. In this study, the immunogenicity of allogeneic MSCs differentiated into new islet β cells was significantly greater than that of new islet β cells derived from GeADSCs, and the low immunogenicity of GeADSCs could be maintained after cell differentiation, which could significantly improve the effect of clinical transplantation treatment. It is highly important to improve the use of these cells in transplantation therapy and tissue engineering.

At present, many researchers have referred to the process of pancreatic development and transdifferentiated MSCs into islet β-like cells through conditioned culture medium or the overexpression of different transcription factors in MSCs [15, 23, 40, 28, 41]). However, many problems remain: one is that there are not enough cells after induction, and the other is that high-maturity islet β cells cannot be obtained. In 2022, the highly effective regulatory gene combination we screened can transdifferentiate fat MSCs into new islet β-cells [6]. In this study, we further optimized the procedure from one transfer of multiple genes to two transfers, and after the transfer of genes, small molecule induction was performed to ensure adequate, more mature newborn islet beta cells. The new islet β cells obtained in this study were tested for a number of biological functions, which confirmed the maturity of the new islet β cells. Single-cell sequencing revealed that multiple genes characteristic of mature islet β cells were highly expressed in each cluster, further demonstrating that the obtained cells were more mature than the previously obtained cells were.

Moreover, the selection of the appropriate transplantation site is also the main factor affecting the clinical success of new islet β-cell transplantation therapy. Yohichi et al. reported that the subcutaneous adipose tissue of the thigh root has strong blood circulation, which is convenient for transplantation operations, conducive to the survival of transplanted cells, and could be used as a cell transplantation site, indicating that the transplantation efficiency of this site was better than that of the liver [36]. Compared with intrasplenic transplantation, intrahepatic transplantation and portal vein transplantation, subcutaneous adipose tissue transplantation at the root of the thigh is simpler and easier to perform, the status of the graft can be detected, and hyperglycemia in the body can be reversed after transplantation to meet treatment needs. Naresh Kasoju et al. implanted a polylactide cocaprolactone (PLCL) capsule scaffold containing the proangiogenic factor VEGF into the omentum of mice and obtained a suitable vascularized pouch 4 weeks later, which could shorten the implantation time of the grafts and prolong their survival time [20]. In this study, before cell transplantation, a fibroin/collagen scaffold was implanted at the transplant site. The implantation of the scaffold formed a vascularized pouch at the transplant site, which could provide living space and nutrition for the cells, shorten the colonization time of the cells, and enable the insulin secreted by the cells to quickly enter the blood circulation and perform biological functions.

Studies on the treatment of diabetes with new islet β cells derived from MSC transplantation are mostly conducted in rodents, and the full effect is rarely observed in other diabetic model animals except mice. Even the therapeutic effect on diabetic model mice is temporary and lacks long-term effects [22, 24, 31]. In this study, we used dogs as experimental animals to explore the effects of cell transplantation therapy on large experimental

animals. On Day 25 after the cells were transplanted into diabetic dogs, the fasting blood glucose of the dogs returned to normal, and they were able to respond to sugar stimulation. In tests of the grafts, it was found that the transplanted cells can express insulin, which can quickly enter the surrounding blood vessels to play a biological role. At the same time, the cells can also migrate to the surrounding fat tissue to secrete insulin. However, in experimental Group 2, blood glucose levels in the dogs began to rise on Day 135 after transplantation, possibly due to transplant rejection. After the transplantation of new islet β cells from normal canine ADSCs + normal canine ADSCs, the numbers of B cells, NK cells, macrophages and cytotoxic T cells at the transplantation site increased significantly, and the levels of cytokines such as IL-1, TNF and M-CSF increased significantly. Parent et al., by completely or selectively knocking out HLA-ABC alleles, created immune-evasive human pluripotent stem cells that reduced the immune response to islet-like beta-cells derived from these cells, a strategy that significantly reduced NK- and T-cell-mediated rejection [25]. In this study, we obtained GeADSCs by knocking out the *B2M* gene and overexpressing the *PD-L1* gene and then obtained islet β-cells with lower immunogenicity. On the 215th day after transplantation, the dogs' blood sugar rose, and the cells remained functioning in the body for longer periods. Compared with those in Experimental Group 2, the numbers of related immune cells and related cytokines were significantly lower, but both were significantly greater than those in the control group. These findings indicate that the low number of immune islet β-cells obtained in this study can significantly improve the clinical therapeutic effect, but further improvement of the antigraft rejection ability of these cells is still necessary. Grafts are protected from host immune cell infiltration through physical barriers, such as the TheraCyte encapsulation device system [9, 30] and alginate hydrogel microcapsules [30]. These physical barriers can support the ability of transplanted cells to maintain cell behavior and protect the graft from the infiltration of inherent immune cells. These factors may be one of the ways to further solve the problem of cell transplantation rejection.

Conclusion

In this study, the B2M gene was knocked out via gene editing technology to cooperate with PD-L1 gene overexpression, and safe GeAMSCs with biological characteristics no difference from those of normal canine ADSCs were obtained, with significantly reduced immunogenicity and enhanced immune escape ability. The optimized induction program can induce the differentiation of MSCs into more mature islet β-cells, and the differentiation of GeAMSCs into newborn islet β-cells can maintain low immunogenicity. Before cell transplantation, a stent can be implanted to form a vascularized pouch at the transplant site to shorten the cell colonization time. After transplantation of low-immunogenicity cells for the treatment of diabetic dogs, the therapeutic effect and antirejection ability of transplantation significantly increased. We hope that these results provide a theoretical and technical reference for solving the problem of transplantation rejection in ADSCs or their post-differentiation.

Supplementary Information

The online version contains supplementary material available at https://doi.org/10.1186/s13287-024-04067-7.

Additional file 1.
Additional file 2.
Additional file 3.
Additional file 4.
Additional file 5.
Additional file 6.
Additional file 7.
Additional file 8.
Additional file 9.
Additional file 10.
Additional file 11.
Additional file 12.
Additional file 13.
Additional file 14.
Additional file 15.
Additional file 16.

Acknowledgements

The authors would like to thank the Experimental Animal Center of Northwest A&F University for providing test animal, the LC-Bio Technology CO., Ltd. for their help in sequencing, and the American Journal Experts (AJE) for helping with English writing. The authors declare that they have not use AI-generated work in this manuscript.

Author contributions

Pengxiu Dai, Yi Wu, Qingjie Du, Methodology, Data curation, Writing-original draft, Writing-review & editing. Juanjuan Du, Keyi Wang, Ruiqi Chen, Collection and/or assembly of the data. Xiancheng Feng, Chen Chen, Provision of study material. Xinke Zhang, Conception and design, Financial support and Manuscript writing.

Funding

This work was supported by 2023 Animal Epidemic Prevention project (Grant No. K3031223086) and Shaanxi Province postdoctoral research project second-class funding (Grant No. 2023BSHEDZZ144).

Availability of data and materials

The datasets generated and/or analysed during the current study are available in the GEO Series with GSE267867 (https://www.ncbi.nlm.nih.gov/geo/query/acc.cgi?acc=GSExxx).

Declarations

Ethics approval and consent to participate

The study is reported in accordance with ARRIVE guidelines (https://arriveguidelines.org). All of the dogs were reared, obtained, and housed in accordance with our institute's laboratory animal requirements. All procedures and the study design were conducted in accordance with the Guide for the Care and Use of Laboratory Animals (Ministry of Science and Technology of China, 2006) and were approved by the Animal Ethical and Welfare Committee of Northwest Agriculture and Forest University (Title of the approved project: Study on anti-graft rejection effect and mechanism of canine gene-edited MSCs and their differentiated cells. Date of approval: September 17, 2022. Approval No: 20220182). No human cells/tissues/samples/cell lines were used in this study.

Consent for publication

Not applicable.

Competing interests

The authors declare no competing interests.

Author details

[1]The College of Veterinary Medicine, Northwest Agriculture and Forestry University, Shaanxi 712100, Yangling, China. [2]MOA Key Laboratory of Animal Virology, Center for Veterinary Sciences, Zhejiang University, Hangzhou 310058, Zhejiang, China. [3]Department of Veterinary Medicine, College of Animal Sciences, Zhejiang University, Hangzhou 310058, Zhejiang, China.

Received: 27 September 2024 Accepted: 19 November 2024
Published online: 02 December 2024

References

1. Barrachina L, et al. Allo-antibody production after intraarticular administration of mesenchymal stem cells (MSCs) in an equine osteoarthritis model: effect of repeated administration, MSC inflammatory stimulation, and equine leukocyte antigen (ELA) compatibility. Stem Cell Res Ther. 2020;11(1):52.
2. Berglund AK, Schnabel LV. Allogeneic major histocompatibility complex-mismatched equine bone marrow-derived mesenchymal stem cells are targeted for death by cytotoxic anti-major histocompatibility complex antibodies. Equine Vet J. 2017;49(4):539–44.
3. Butler A, et al. Integrating single-cell transcriptomic data across different conditions, technologies, and species. Nat Biotechnol. 2018;36(5):411–20.
4. Castro-Gutierrez R, et al. Protecting Stem Cell Derived Pancreatic Beta-Like Cells From Diabetogenic T Cell Recognition. Front Endocrinol (Lausanne). 2021;12:707881.
5. Dai P, et al. Novel functional genes involved in transdifferentiation of canine ADMSCs into insulin-producing cells, as determined by absolute quantitative transcriptome sequencing analysis. Front Cell Dev Biol. 2021;9:685494.
6. Dai P, et al. Reprogramming adipose mesenchymal stem cells into islet β-cells for the treatment of canine diabetes mellitus. Stem Cell Res Therapy. 2022;13(1):370.
7. Damrich S, et al. Visualizing single-cell data with the neighbor embedding spectrum. bioRxiv. 2024. https://doi.org/10.1101/2024.04.26.590867.
8. Demeester S, et al. HLA-A*24 carrier status and autoantibody surges post-transplantation associate with poor functional outcome in recipients of an islet allograft. Diabetes Care. 2016;39(6):1060–4.
9. El-Halawani SM, et al. Subcutaneous transplantation of bone marrow derived stem cells in macroencapsulation device for treating diabetic rats; clinically transplantable site. Heliyon. 2020;6(5):e03914.
10. Fein JA, et al. Systematic evaluation of donor-KIR/Recipient-HLA Interactions in HLA-matched hematopoietic cell transplantation for AML. Blood Adv. 2023;8(3):581.
11. Gao LL, et al. Irrigating degradation properties of silk fibroin-collagen type II composite cartilage scaffold in vitro and in vivo. Biomater Adv. 2023;149:213389.
12. Ghosh C, et al. A snapshot of the PD-1/PD-L1 pathway. J Cancer. 2021;12(9):2735–46.
13. Godsland IF, et al. The importance of intravenous glucose tolerance test glucose stimulus for the evaluation of insulin secretion. Sci Rep. 2024;14(1):7451.
14. Halm D, et al. Direct comparison of the immunogenicity of major histocompatibility complex-I and -II deficient mesenchymal stem cells in vivo. Biol Chem. 2021;402(6):693–702.
15. Hashemi Tabar M, et al. The combined effect of Pdx1 overexpression and Shh manipulation on the function of insulin-producing cells derived from adipose-tissue stem cells. FEBS Open Bio. 2018;8(3):372–82.
16. Hu J, et al. Blockade of STARD3-mediated cholesterol transport alleviates diabetes-induced podocyte injury by reducing mitochondrial cholesterol accumulation. Life Sci. 2024;349:122722.
17. Huang X, et al. scAnnoX: an R package integrating multiple public tools for single-cell annotation. PeerJ. 2024;12:e17184.
18. Huang Y, Wu Q. Immunomodulatory mechanisms of mesenchymal stem cells and their potential clinical applications. Int J Molecular Sci. 2022;23(17):10023.
19. Kanehisa M, et al. KEGG for linking genomes to life and the environment. Nucleic Acids Res. 2008;36:D480-484.
20. Kasoju N, et al. Bioengineering a pre-vascularized pouch for subsequent islet transplantation using VEGF-loaded polylactide capsules. Biomater Sci. 2020;8(2):631–47.
21. Liu LP, et al. Netrin-1 prolongs skin graft survival by inducing the transformation of mesenchymal stem cells from pro-rejection to immune-tolerant phenotype. Eur Rev Med Pharmacol Sci. 2019;23(20):8741–50.
22. Lumelsky N, et al. Differentiation of embryonic stem cells to insulin-secreting structures similar to pancreatic islets. Science. 2001;292(5520):1389–94.
23. Ohta S, Ikemoto T. "A change in the zinc ion concentration reflects the maturation of insulin-producing cells generated from adipose-derived mesenchymal stem cells. Sci Rep. 2019;9(1):18731.
24. Pagliuca FW, et al. Generation of functional human pancreatic β cells in vitro. Cell. 2014;159(2):428–39.
25. Parent AV, et al. Selective deletion of human leukocyte antigens protects stem cell-derived islets from immune rejection. Cell Rep. 2021;36(7):109538.
26. Qin L, et al. Mesenchymal stem cells in fibrotic diseases-the two sides of the same coin. Acta Pharmacol Sin. 2023;44(2):268–87.
27. Rickels MR, Robertson RP. Pancreatic islet transplantation in humans: recent progress and future directions. Endocr Rev. 2019;40(2):631–68.
28. Saghahazrati S, et al. The synergistic effect of glucagon-like peptide-1 and chamomile oil on differentiation of mesenchymal stem cells into insulin-producing cells. Cell J. 2020;21(4):371–8.
29. Su Q, et al. Single-cell insights: pioneering an integrated atlas of chromatin accessibility and transcriptomic landscapes in diabetic cardiomyopathy. Cardiovasc Diabetol. 2024;23(1):139.
30. Tahbaz M, Yoshihara E. Immune protection of stem cell-derived islet cell therapy for treating diabetes. Front Endocrinol (Lausanne). 2021;12:716625.
31. Takahashi H, et al. Regenerative and transplantation medicine: cellular therapy using adipose tissue-derived mesenchymal stromal cells for type 1 diabetes mellitus. J Clin Med. 2019;8(2):249.
32. Talayev VY, et al. The effect of human placenta cytotrophoblast cells on the maturation and T cell stimulating ability of dendritic cells in vitro. Clin Exp Immunol. 2010;162(1):91–9.
33. van Megen KM, et al. Activated mesenchymal stromal cells process and present antigens regulating adaptive immunity. Front Immunol. 2019;10:694.
34. Wang H, et al. Beta2-microglobulin(B2M) in cancer immunotherapies: Biological function, resistance and remedy. Cancer Lett. 2021;517:96–104.
35. Wang Y, et al. Reciprocal regulation of mesenchymal stem cells and immune responses. Cell Stem Cell. 2022;29(11):1515–30.
36. Yasunami Y, et al. A Novel Subcutaneous Site of Islet Transplantation Superior to the Liver. Transplantation. 2018;102(6):945–52.
37. Yin Z, et al. Skin proteomic screening and functional analysis of differential proteins associated with coat color in sheep (Ovis aries). Anim Biosci. 2024;37:1503.
38. Zangi L, et al. Direct imaging of immune rejection and memory induction by allogeneic mesenchymal stromal cells. Stem Cells. 2009;27(11):2865–74.

39. Zhang G, et al. A novel accelerated rejection model for mouse cardiac transplantation involving presensitization with donor splenocytes. J Surg Res. 2013;181(1):146–55.
40. Zhang T, et al. Pax4 synergistically acts with Pdx1, Ngn3 and MafA to induce HuMSCs to differentiate into functional pancreatic β-cells. Exp Ther Med. 2019;18(4):2592–8.
41. Zhang Y, Gao S. Exendin-4 gene modification and microscaffold encapsulation promote self-persistence and antidiabetic activity of MSCs. Sci Adv. 2021. https://doi.org/10.1126/sciadv.abi4379.

Publisher's Note